Prediction of the Aerodynamic Sound Power Level of a High Speed Train Bogie Based on Unsteady FW-H Simulation

Martin Rissmann, Romain Leneveu, Claire Chaufour, Alexandre Clauzet, and Fabrice Aubin

Abstract Aerodynamic noise is generated by interaction of the air flow with an object and by the turbulent flow itself. In railways it becomes a significant noise source for speeds above 250 kph and major areas of noise generation on (high speed) trains are the train head, the leading and second bogie, the pantograph and the gaps between coaches. This paper presents a numerical simulation approach based on CFD/CAA techniques aiming to estimate equivalent sources for aerodynamic noise of different components of SNCF's TGV high speed trains. The approach is based on an unsteady DES flow simulation combined with the Ffowcs-Williams and Hawkins (FW-H) analogy for the acoustic part. In order to develop the method a symmetric and full model are implemented and the leading bogie was selected as an application case. Results of this simulation, in terms of sound power and directivity, are already used by SNCF noise experts in order to estimate pass-by noise levels of TGV high speed trains. In the future other noise source will be simulated and mitigation devices such as deflectors will be tested numerically.

Keywords Aeroacoustics · High speed train · FW-H

1 Introduction

Railway noise is largely dominated by rolling noise. However, above 250–300 kph and beyond, the aerodynamic noise becomes a significant additional source, which can even become the dominant noise source. It is characterized by an evolution with speed following 60–80 log laws and its tonal components and broadband character in the low and mid-frequency range [1]. The noise is generated by interaction of the

M. Rissmann (✉) · R. Leneveu
Vibratec, Railway Business Unit, 28 Chemin du Petit Bois, 69130 Ecully Cedex, France
e-mail: martin.rissmann@vibratec.fr

C. Chaufour · A. Clauzet · F. Aubin
SNCF Voyageurs—SNCF Materiel Ingénierie du Matériel—Centre d'Ingénierie du Matériel, 4, Allée des Gémeaux, 72100 Le Mans, France

air flow with the train surfaces and by the turbulent flow itself (turbulent boundary layer, un-steady wake, etc.). It is well known from several publications [2–7] that the major aerodynamic noise sources are the train head, the leading and second bogie, the pantograph and the gap between trailers.

For SNCF the main goal is to be able to estimate aerodynamic noise sources in order to include them in exterior noise emission predictions at train level (including rolling and equipment noise sources) for typical EMU running at 200 kph and more. Further-more once the noise emission of the whole train is simulated, SNCF is able to define the source term for the CNOSSOS noise assessment method (European parliament directive 2002/49/CE).

2 Methodology

SNCF uses STARCCM+ for different aerodynamic simulations. Therefore in this study, this tool is used for the prediction of the aerodynamic sound power of the leading bogie. The prediction approach is based on an unsteady DES aerodynamic flow simulation combined with the Ffowcs-Williams and Hawkins (FW-H) analogy for far-field acoustic prediction. To ensure a correct implementation of the approach in STARCCM+ the well-known reference case of flow noise around a tandem cylinder was reproduced before modelling the TGV train: Satisfying agreement with the simulated and measured reference case was obtained [8].

2.1 Setup

Figure 1 shows the computation domain with the TGV train's head: the nose is placed far from the inlet boundary condition such that the flow field develops properly. The bogie geometry is modelled in detail including suspension elements, brake discs, motors and gearboxes. After the first bogie the train's geometry is simplified by extruding its section up to the outlet boundary condition. Furthermore, two numerical models are created: A first model comprises a symmetry plane along the center axis of the train to save computation time. This hypothesis is acceptable with regard to the objective of the project. A second model takes into account the full train geometry.

Both models have a trimmed mesh with a base size of 0.56 m, which is refined towards the bogie area, where a cell size of 8.4 mm is reached, see Fig. 2. More details about the mesh parameters and the boundary conditions are given in Tables 1 and 2. The chosen mesh resolution allows to solve turbulence (local turbulent fluctuations compared to mesh size) up to 500 Hz (symmetric model), respectively 1000 Hz for the acoustic part (at least 20 elements per wavelength). For the full model turbulence is resolved up to 800 Hz and acoustics up to 2000 Hz.
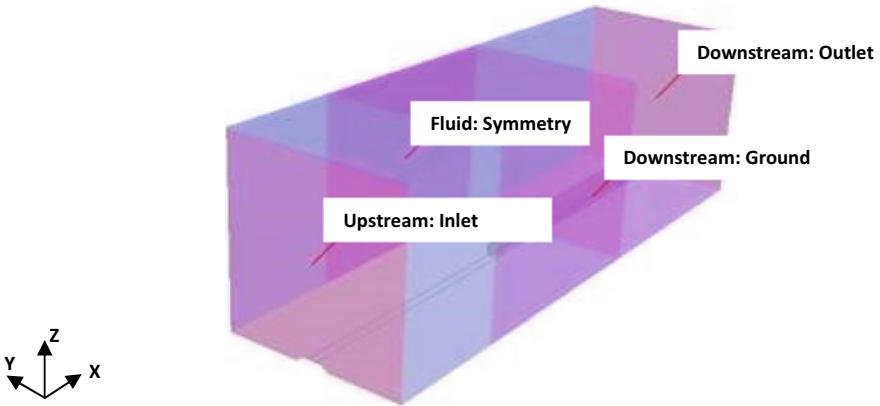
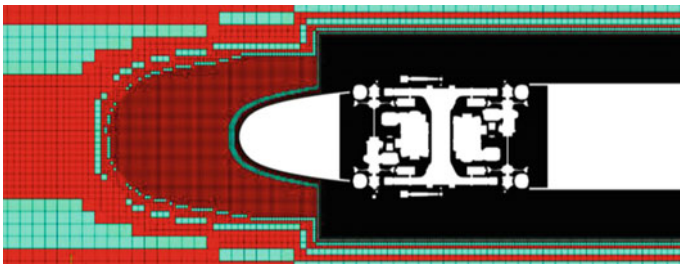**Fig. 1** Computation domain and boundaries—X = longitudinal, Y = lateral, Z = vertical

Fig. 2 Computation mesh in a horizontal plane 1.5 m above ground—full model

Table 1 Mesh parameters

Parameter	Symmetric model	Full geometry
Domain length (X)	20 m upstream extension + 37.75 m + 40 m downstream extension	
Domain width (Y)	10 m	30 m
Domain height (Z)	25 m	30 m
Total number of cells	36 millions	167 millions
Boundary layers	6	10
1st layer thickness		2e−5 m
Boundary layer thickness		4.4 mm

2.2 FW-H

The sound pressure at far-field receivers is predicted using the FW-H acoustic analogy with Farrassat's Formulation 1A. Two FW-H source regions are defined: The first

Table 2 Boundary conditions

Boundary	Value
Inlet	Velocity inlet 320 km/h
Outlet	Pressure outlet
Ground	Wall—no slip
Sides	Symmetry
Y = 0	Symmetry
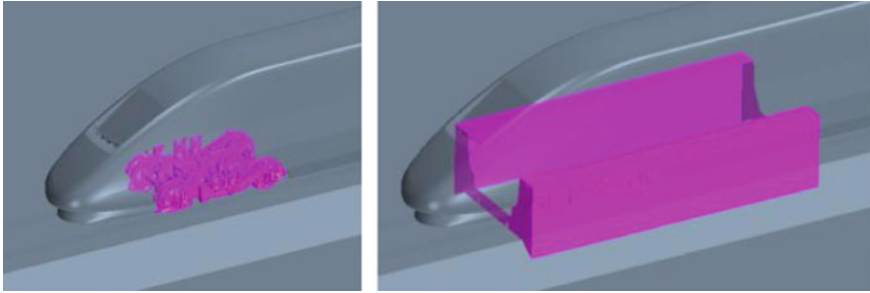
Fig. 3 Left: Impermeable FW-H surface—right: permeable FW-H surface

one, so called impermeable surface, takes into account the skin of the bogie, which corresponds to free-field radiation, see Fig. 3 left. The second one, is a so-called permeable surface allowing to take into account acoustic interaction in the bogie cavity, see Fig. 3 right. The back surface in downstream direction of this FW-H source is not considered in the evaluation since it is known that artificial, spurious signals might appear [9]. The mesh size in the permeable FW-H is 8.4 mm for both models, which makes this region computationally expensive. FW-H volume terms (quadrupole noise), which take into account nonlinearities in the flow and are computationally expensive, are not considered.

2.3 Numerical Resolution

The numerical resolution of the problem consists of three steps: First the flow field is initialized with a steady RANS model. Then, in the second step, the unsteady flow field, resolved by a DES model, is initiated in order to develop the turbulent flow before activating in the third step the FW-H model with a smaller time step, see details in Tables 3 and 4.

For the symmetric model, pressure signals at virtual microphone positions are recorded at a frequency of 5.1 kHz starting from 0.6 s physical time. The chosen approach for the symmetric model is aggressive since only one flow flush between the train nose and the end of the bogie zone (estimated time 0.09 s) is considered

Table 3 Physical time section and time steps

Parameter	Symmetric model	Full model
Physical time flow initialization (s)	0–0.5	0–1.4
Time step initialization (s)	1e−3	1e−3
Physical time FW-H resolution (s)	0.5–0.75	1.4–1.75
Time step FW-H (s)	6.5e−5	4e−5

Table 4 Model and solver parameters

| Parameter	Value
Turbulence	K-omega SST
Gas	Ideal gas
Solver	Segregated flow and fluid temperature
Numerical scheme	2nd order implicit
Iterations per times step	Min. 5–max. 10

before starting signal recording. This choice is made in order to meet the major aim of the project which consisted in implementing the complete approach up to the equivalent noise source. For the full model, a less aggressive approach was chosen.

2.4 Post-Processing

For each virtual microphone pressure signals are either recorded directly (FW-H on the fly) or in a post-FW-H approach for a duration of 0.125 s (symmetric model). For the later, the necessary flow field data is exported during the computation run. This approach has the advantage that microphone positions do not have to be defined before-hand.

The equivalent acoustic source of the bogie is described by the sound power and directivity which are both determined using a virtual microphone array, see Fig. 4. The sound power is obtained from the mean pressure of 40 microphones arranged regularly on a hemisphere around the bogie center (ISO 3745 standard). For the symmetric model, the pressure signals from the modelled side are mirrored to the non-modelled, symmetric side. Furthermore, ground effects are not considered.

Fig. 4 Virtual microphone array used to determine the equivalent acoustic source of the bogie
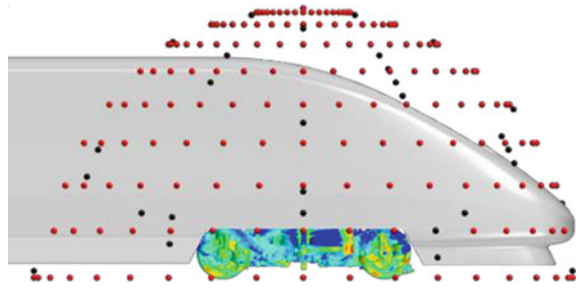
3 Results

3.1 Flow Field

The aerodynamic part of the model is validated by comparing the drag force to previously obtained results of a numerical simulation with Powerflow [10]. A good agreement is observed such that the model is validated from this point of view. Furthermore the drag force is compared between the different model implementations as shown in Fig. 5: A good agreement is observed; the main effects on drag such as the impact of the nose and bogie are well reproduced by all models.

A snapshot of the instantaneous velocity field in the bogie area, see Fig. 6, reveals the turbulent nature of the flow: First the flow is slowed down up to the stagnation point at the nose, before being accelerated below and along the car body. Strong flow-structure interaction, mainly observed at the axle box of the first wheelset and the longitudinal damper, causes formation of turbulent eddies combined with strong velocity gradients.

Aerodynamic noise sources are related to instantaneous pressure fluctuations p' $= p - \bar{p}$ as shown in Fig. 7. The main fluctuations in the shown plane are located at the previously identified regions of strong flow-structure interaction, see Fig. 6:

Fig. 5 Comparison of drag forces between RANS and instantaneous DES results for the symmetric and full model
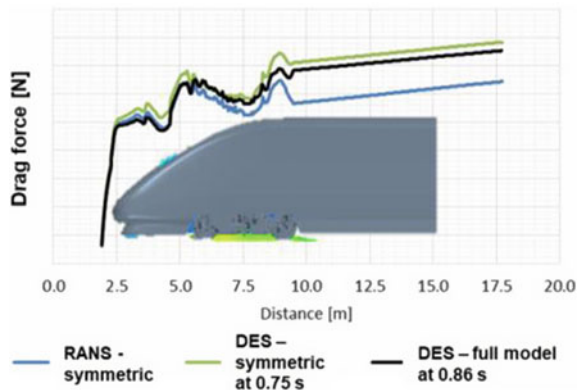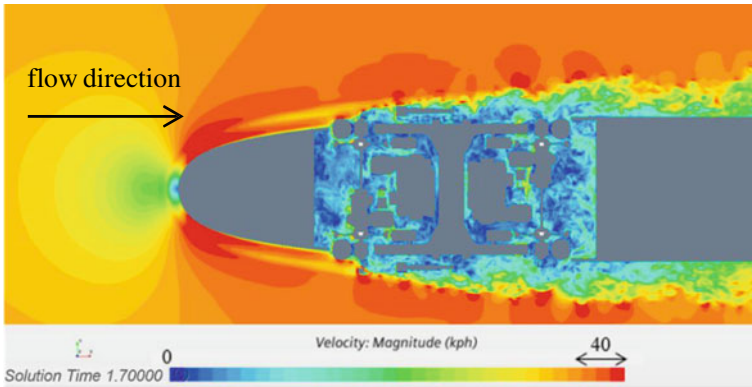
Fig. 6 Instantaneous velocity magnitude in a horizontal plane 1.5 m above ground—full model
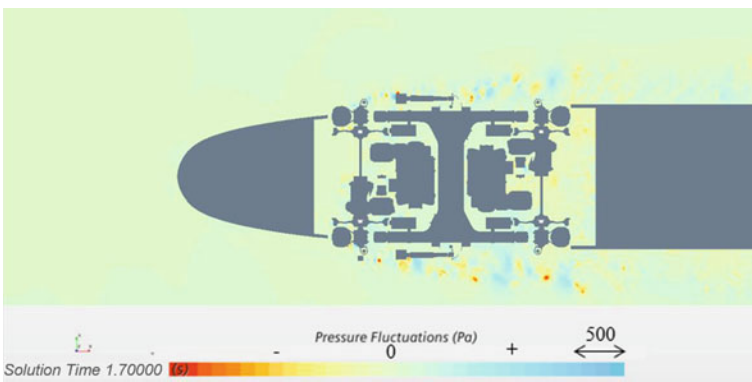

Fig. 7 Instantaneous pressure fluctuations p′ in a horizontal plane 1.5 m above ground—full model

The axle box of the first wheelset and the longitudinal damper are both elements that protrude above the car body envelope.

3.2 Acoustics

Currently, acoustic results are only available for the symmetric model: Fig. 8 shows the sound power spectra of the two FW-H source regions: taking into account the bogie cavity (permeable region) leads to a 5 dB lower noise level. Furthermore the spectra reveal two emerging third octave bands at 250 and 500 Hz third octave band, which are probably related to flow-structure interaction in the region of the axle box and longitudinal damper (see Figs. 6 and 7). Both bands were previously observed

Fig. 8 Sound power—full
line: impermeable FW-H
source—dashed line:
permeable FW-H
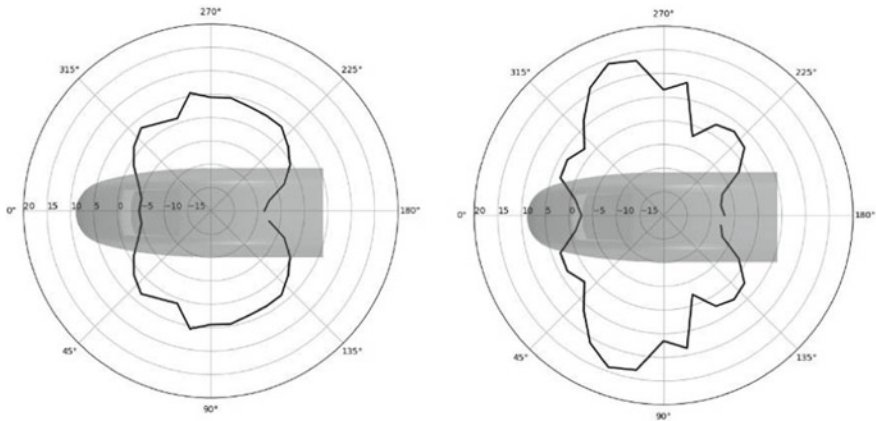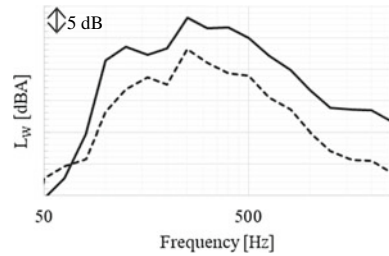source—symmetric model

Fig. 9 Horizontal directivity (dB) in the 250 Hz band of the symmetric model—left: impermeable FW-H source surface—right: permeable FW-H source surface—symmetric model

by SNCF in numerical simulations and measurement campaigns, so the results of this work can be trusted.

Figure 9 shows the directivity patterns in horizontal direction of both FW-H sources in the 250 Hz third octave band. The directivity from the modelled side is mirrored to the non-modelled side. The leading bogie has a dipole radiation characteristic in the horizontal plane.

4   Conclusions

In this work a numerical simulation approach based on CFD/CAA techniques is developed to predict aerodynamic noise of different components of SNCF's TGV high speed trains. The approach is applied to estimate an equivalent acoustic source for the first, leading bogie. First acoustic results, obtained with a symmetric, computationally less expensive model are presented. The results reveal that the leading bogie has a dipole characteristic with emerging frequencies in the 250 and 500 Hz third octave band, which was also observed in previous works by SNCF. Using two

different FW-H source zones allows to show that the bogie cavity acts as an acoustic screen and influences the source directivity.

In a next step, the results will be compared to the full model which has also a higher resolution. This allows to see if the computationally less expense symmetric approach is sufficient to estimate an equivalent acoustic source for the aerodynamic noise. In addition to that the aerodynamic noise will be compared to rolling noise, which is another major railway noise source.

In the future the suggested approach will allow SNCF to estimate other aerodynamic noise sources such as the pantograph recess, the inter coach gap and the second bogie for example. Also, the impact of noise mitigation devices such as flow deflectors can be quantified before actual prototype tests.

Finally, the results from this work are already used by SNCF noise experts in order to predict the exterior noise emission of TGV high speed trains.

References

1. Thompson D (2008) Railway noise and vibration: mechanisms, modelling and means of control. Elsevier
2. Mellet C, Létourneaux F, Poisson F, Talotte C (2006) High speed train noise emission: latest investigation of the aerodynamic/rolling noise contribution. J Sound Vib 293(3–5):535–546
3. Poisson F (2013) Railway noise generated by high-speed trains. In: Proceedings of the 11th international workshop on railway noise. Uddevalla
4. Zhang J et al (2018) Source contribution analysis for exterior noise of a high-speed train: experiments and simulations. Shock Vib 2018:1–13
5. Li C, Chen Y, Xie S, Li X, Wang Y, Gao Y (2021) Evaluation on aerodynamic noise of high speed trains with different streamlined heads by LES/FW-H/APE method. In: Noise and vibration mitigation for rail transportation systems. Springer, pp 57–65
6. Minelli G, Yao HD, Andersson N, Höstmad P, Forssén J, Krajnović S (2020) An aeroacoustic study of the flow surrounding the front of a simplified ICE3 high-speed train model. Appl Acoust 160:107–125
7. Iglesias EL, Thompson DJ, Smith MG (2015) Component-based model for aerodynamic noise of high-speed trains. In: Noise and vibration mitigation for rail transportation systems. Springer, pp 481–488
8. Lockard D (2011) Summary of the tandem cylinder solutions from the benchmark problems for airframe noise computations-I workshop. In: 49th AIAA aerospace sciences meeting including the new horizons forum and aerospace exposition, p 353
9. Lopes LV et al (2017) Identification of spurious signals from permeable Ffowcs-Williams and Hawkings surfaces. In: American Helicopter Society (AHS) international annual forum and technology display, no. NF1676L-25336
10. Masson E, Paradot N, Allain E (2010) The numerical prediction of the aerodynamic noise of the TGV POS high-speed train power car. In: Proceedings of the 10th international workshop on railway noise, Nagahama